

This document is the Accepted Manuscript version of a Published Work that appeared in final form in The Journal of Organic Chemistry, copyright © American Chemical Society after peer review and technical editing by the publisher. To access the final edited and published work see <https://doi.org/10.1021/acs.joc.2c01303>

# One-Pot Synthesis of Pyreno[2,1-b]furan Molecules with Two-Photon Absorption Properties

*Xiaohui Wang,<sup>#a</sup> Chengjing Zhang,<sup>#b</sup> Jin Zeng,<sup>a</sup> Xiaoyu Mao,<sup>a</sup> Carl Redshaw,<sup>c</sup> Guangle Niu,<sup>\*b</sup>*

*Xiaoqiang Yu,<sup>b</sup> Xing Feng<sup>\*a,d</sup>*

<sup>a</sup> Guangdong Provincial Key Laboratory of Information Photonics Technology, School of Material and Energy, Guangdong University of Technology, Guangzhou 510006, P. R. China

<sup>b</sup> Center of Bio and Micro/Nano Functional Materials, State Key Laboratory of Crystal Materials, Shandong University, Jinan 250100, P. R. China.

<sup>c</sup> Department of Chemistry, University of Hull, Cottingham Road, Hull, Yorkshire HU6 7RX, UK.

<sup>d</sup> Guangdong Provincial Key Laboratory of Luminescence from Molecular Aggregates (South China University of Technology), Guangzhou 510640, P. R. China.

**KEYWORDS:** pyrene intermediates, one-pot synthesis, organic luminescent materials, two-photon absorption (TPA) properties.

**ABSTRACT:** The development of large  $\pi$ -conjugated polycyclic heteroaromatic materials is of

immense interest, both in the academic as well as the industrial community. Herein, we present the efficient one-pot synthesis of novel pyreno[2,1-b]furan molecules from a newly designed intermediate, which display intense green emission (505-516 nm) in solution and a large red shift emission (625-640 nm) in the solid state, due to strong  $\pi$ - $\pi$  stacking. More interestingly, the compounds exhibit novel two-photon absorption (TPA) properties and the TPA cross section ( $\delta$ ) value was increased to 533 GM by regulating the electronic effects of the substituents of the pyreno[2,1-b]furan molecules. This study not only offers a facile strategy for constructing new pyrene fused luminescence materials with two-photon absorption properties, but also provides a new chemical intermediate that opens up a new pathway to advanced materials.

## 1. Introduction

Pure organic  $\pi$ -conjugated luminescence molecules have attracted intense interest because of their practical applications in the fields of organic electronics, nonlinear optics, energy storage devices,<sup>1 2</sup> and bioimaging.<sup>3 4</sup> In recent years, much effort has been devoted to the construction of multi-functional organic luminescence materials with blue/green/red (RGB) emission. Moreover, organic fluorophores with two-photon absorption (TPA) properties exhibit unique advantages for cell imaging, biomedical diagnosis and therapy, due to their long excitation wavelengths, less photobleaching, higher 3D resolution and penetration depths.<sup>5</sup> The main strategy for developing the TPA properties of organic luminescent materials is to explore their donor-acceptor (D-A) structures, and the electronic push-pull capability, whilst the length of  $\pi$ -conjugation and planarity of the  $\pi$ -center play a

crucial role in improving the TPA cross sections ( $\delta$ ).<sup>6</sup> However, facile access to organic luminescent materials with tuneable emission color, high fluorescence yield, and a high TPA cross sections remains a challenge.

Pyrene, a four ring fused polycyclic aromatic hydrocarbon (PAH) with  $\pi$ -center characteristics, possesses good thermal stability, high carrier mobility, and intensive blue emission with high fluorescence efficiency.<sup>7 8</sup> Thus, pyrene-based derivatives are an important building block not only for exploring high performance *n*-type organic semiconductors,<sup>9</sup> but also are widely used as organic luminescent materials for organic light emitting diodes (OLEDs),<sup>10</sup> and fluorescent probe applications. On the other hand, it is very popular to prepare pyrene-based D-A molecules with intriguing optoelectronic properties via a rational molecular design. For example, Klaus reported a multi-step synthetic protocol to asymmetrically functionalize pyrene at the 4,5- and 9,10-positions, to afford a red luminescent molecule (613 nm) via tuning of the HOMO-LUMO gap to 2.26 eV.<sup>11</sup> Moreover, our group presented new pyrene-based dipolar molecules via controllable regioselective substitution at the 1,3- and 6,8- (or 5,9-) positions of pyrene, which exhibited wide tuneable emission over the range from blue (437 nm) to orange-red (571 nm) in solution. More importantly, there is no doubt that expanding the  $\pi$ -conjugation molecular skeletons of pyrene with suitable D-A substituents is an available method to achieve novel TPA properties<sup>6 12 13</sup> and long wavelength emission fluorescent materials.<sup>14</sup> However, pyrenes possessing more  $\pi$ -conjugated aromatic rings not only suffer from decreased air

stability, solubility and fluorescence properties, but also are increasingly difficult to synthesize.

Polycyclic heteroaromatics are an important class of  $\pi$ -conjugated compounds, where the molecular skeletons containing N, O or B atom can enhance the thermal/air stability and tuneable optoelectronic properties, as well as increase the electron affinity. Liu *et al.* reported a series of pyrene-fused thioxanthenes, which possessed a high HOMO level and a narrow energy gap.<sup>15</sup> Moreover, Liu proposed novel *n*-type pyrene-based azaacenes via incorporating boron–nitrogen coordination bonds at the pyrene core, which exhibited low-lying LUMO energy levels and high electron affinities with electron mobility of  $\sim 1.60 \text{ cm}^2 \text{ V}^{-1} \text{ s}^{-1}$ .<sup>16 17</sup> Meanwhile, the K-region of pyrene-fused furan derivatives is not only used to access synthetic intermediates,<sup>18</sup> but also to afford excellent blue light materials for OLEDs.<sup>19 20 21</sup> It is noteworthy that the arylethynyl group when at the 1,3,6,8-positions of pyrene can influence the  $S_1 \leftarrow S_0$  and  $S_3 \leftarrow S_0$  transitions,<sup>18</sup> and lead to emission across the visible region.<sup>22</sup> Recently, our group synthesized a new pyrene-based intermediate 1,3,6,8-tetrabromo-2-hydroxypyrene (**1**) for the preparation of solid-state dual emission materials.<sup>23</sup> It was found that the 1-, 3-, 6- and 8- substituted alkynylpyrene derivatives exhibited marked electrogenerated chemiluminescence,<sup>24</sup> and TPA properties with a large  $\delta$  value.<sup>6</sup> We were inspired by the knowledge that 2-(4-methoxyphenyl)benzofuran (**MBF**) can be accessed via two synthetic steps involving a Pd-catalyzed Sonogashira reaction and a cyclization reaction using a 2-bromophenol precursor albeit in a relatively low yield,<sup>25</sup> which also can be achieved by a one-step synthesis using specific palladium catalysts

(Scheme 1).<sup>26</sup> Thus, the key intermediate **1** could also allow for the formation of pyreno[2,1-b]furan molecules with excellent optical properties. With this in mind, we describe herein a facile, one-pot synthesis of a series of novel pyreno[2,1-b]furan derivatives **2a-c** and **3** which exhibit excellent optical behavior with TPA properties. More importantly, we successfully regulated the two-photon absorption cross section ( $\delta$ ) value up to 533 GM via introducing electron donating groups. To the best of our knowledge, this is the first example to achieve highly efficient luminescent materials by expanding the  $\pi$ -conjugated pyrene skeleton using a one-step classical synthetic reaction.

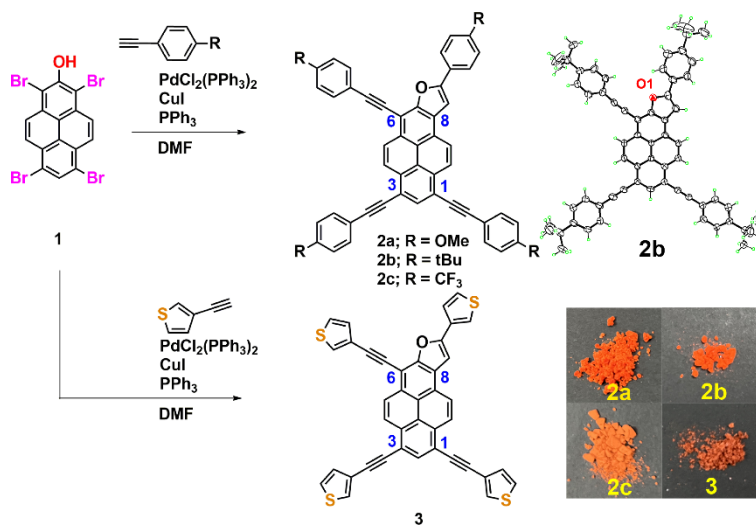
## 2. Results and discussion

### 2.1 Synthesis and characterization

According to Scheme 1, the pyreno[2,1-b]furan molecules **2** and **3** were synthesized by a one-pot synthesis using a Pd-catalyzed Sonogashira coupling reaction in high yield. The structures of all compounds were confirmed by <sup>1</sup>H/<sup>13</sup>C NMR spectra, high resolution mass spectrometry (HRMS), as well as by single crystal X-ray diffraction analysis. The substituents (such as the 4-methoxyphenylethynyl, 4-(*tert*-butyl)phenylethynyl, trifluoromethylphenyl, ethynylthiophenyl) were selected for regulating the electron effect in order to optimize the optical behavior. However, the expanding  $\pi$ -conjugated compounds display a relatively low solubility in organic solvents, and did not dissolve in water.

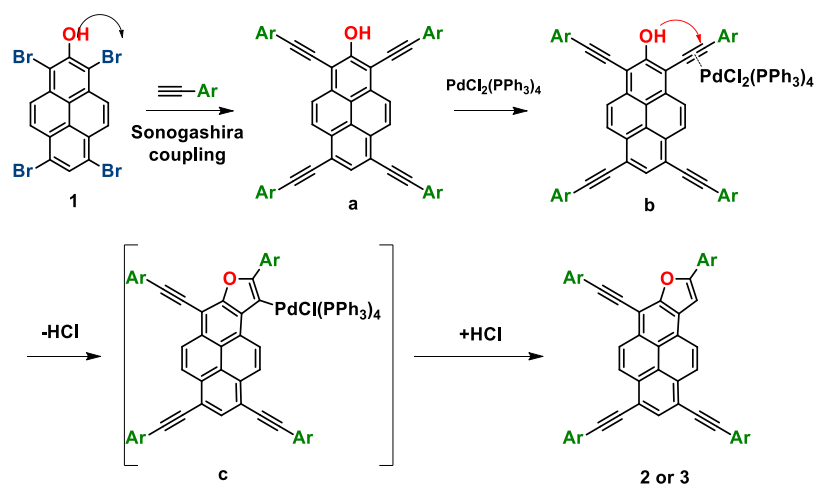
Based on our experiments, if the substituted group occupies the 1,3,6,8-positions of pyrene, the symmetric molecules would show simple <sup>1</sup>H NMR proton peaks at low field in

the region 8.2-9.0 ppm, whilst the proton signal for the -OH is located at 5.36 ppm. However, considering **2b** as an example, four pairs of double proton peaks at  $\delta$  8.71, 8.64, 8.59, 8.34 and a singlet peak at 8.31 ppm respectively, with integrations of 1:1:1:1:1 are observed, while the singlet peak for the -OH has disappeared, implying that the target compound **2b** possesses an unsymmetric structure. (Figure S4) Moreover,  $^1\text{H}$ - $^1\text{H}$  NOSEY NMR spectroscopy of **2** and **3** was performed to confirm the molecular structures. In the case of **2b**, the single peak at 7.62 ppm was assigned to the proton at the furan ring, which correlates with the double peak at 7.51 ppm from the proton of the phenyl ring (Figure S14). Thus, both NMR spectroscopy and the HRMS are in agreement with a pyreno[2,1-b]furan structure.



**Scheme 1.** Synthetic route to pyreno[2,1-b]furan molecules **2** and **3**; top right: ORTEP drawing of crystal **2b**. the ellipsoid probability is 30%; insert: the compounds **2** and **3** under daylight.

Fortunately, single crystals of **2b** (CCDC: 2166623) suitable for X-ray crystallography were cultivated from CHCl<sub>3</sub> solvent, which were not stable under air (the small size of crystals led to weak diffraction and high R indices). The X-ray crystallographic analysis provides direct evidence to confirm the exact structure of the pyreno[2,1-b]furan molecule **2b**. The crystal of **2b** crystallizes in the triclinic system with a P-1 space group. The compound **2b** forms an almost co-planar molecular framework with a dihedral angle of ~30.27 ° between the pyreno[2,1-b]furan core and the 4-(*tert*-butyl)phenylethynyl units. Moreover, the molecule adopts a face-to-face  $\pi$ - $\pi$  interaction with a distance of 3.38 Å, (Figure S21) indicating that the compounds prefer to form a dimer in the aggregated state or in the solid state.



**Scheme 2.** The proposed mechanism of the one-pot synthesis of pyreno[2,1-b]furan molecules **2** and **3**.

Previously, the metal-catalyzed cyclization reaction of *o*-alkynyl phenols to benzofurans have been summarized.<sup>27</sup> Following these reports, a plausible reaction mechanism for the Pd-catalyzed one-pot synthesis of pyreno[2,1-b]furan has been proposed

in Scheme 2.<sup>28,29,30,31</sup> The mechanism of the Pd-catalyzed Sonogashira coupling reaction to arylethynyl was thoroughly investigated. We speculate that a Pd-catalyzed coupling reaction of the pyrene-based precursor **1** affords the symmetric compound **a**. Then, the Pd(II)-catalyzed cyclization occurred via attack of the triple bond to form the pyreno[2,1-b]furan intermediate **c**. Following, protonation of the intermediate **c**, the compounds **2** or **3** were afforded.<sup>25,32</sup>

## 2.2 UV-vis and fluorescence spectra

The photophysical properties of **2** and **3** were investigated in dilute THF solution ( $\sim 10^{-5}$  M) at room temperature, and their corresponding photophysical data are summarized in Table 1. As shown in Figure 1A, the UV-vis spectra of the four compounds exhibited similar absorption behavior, *i.e.* two distinct absorption bands are located in the range 300-370 nm and 400-525 nm, respectively. The short-wavelength absorption band can be assigned to a vibronic feature characteristic of the  $\pi$ -conjugated pyreno[2,1-b]furan skeleton absorption, and the long-wavelength absorption band originates from characteristic  $n-\pi^*$  transitions. Clearly, the maximum long-wavelength absorption band of compounds **2** and **3** are more than 10 nm red shifted compared to 1,3,6,8-tetrakis[(4-methoxyphenyl)ethynyl]pyrene,<sup>22</sup> which may be ascribed to the expanded  $\pi$ -conjugated pyreno[2,1-b]furan core. Additionally, among the four compounds, **2a** displayed the largest absorption wavelength ( $\lambda_{\text{abs}} = 495$  nm), which can be attributed to the methoxy group having the strongest electron-donating ability of the four different substituents. With the substituents replaced by ethynylthiophenyl units, compound **3** exhibits a higher molar



absorption coefficient of  $\epsilon = 1.15 \times 10^5 \text{ M}^{-1} \text{ cm}^{-1}$ , indicating that **3** forms a more planar structural conformation with a larger  $\pi$ -conjugation system compared to compound **2**. Furthermore, the absorption of compounds **2-3** were measured in thin films (Figure 1C), and **2a** exhibits a large red shifted absorption peak compared to in solution, while the short wavelength absorption bands of **2b** and **2c** exhibit only slight changes. However, the maximum long wavelength absorption peaks of the compounds were blue shifted to 470 nm for **2b** and 464 nm for **2c**, respectively. In contrast to **2a**, the maximum short wavelength absorption peak of compound **3** was red shifted to 355 nm, and the maximum long wavelength absorption peaks was blue shifted to 472 nm. In addition, the compounds **2a**, **2c** and **3** display a broader absorption band in range 310-800 nm, which may be ascribed to their different molecular packing via intramolecular interactions, such as  $\pi$ - $\pi$  stacking, and hydrogen bonding interactions.

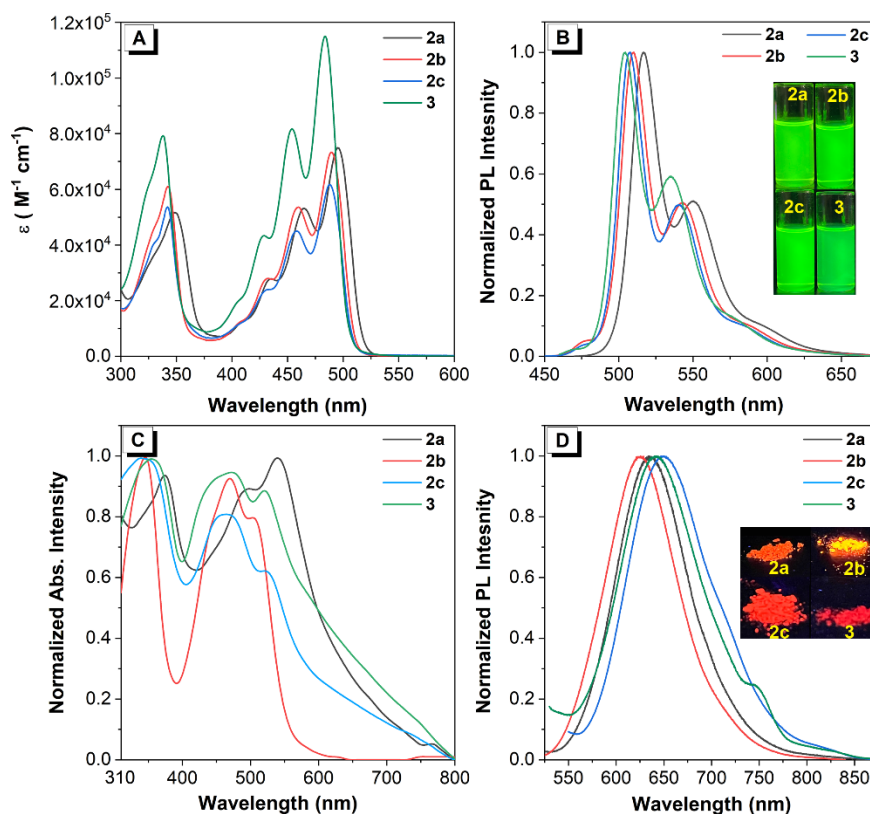


**Figure 1.** (A), (C) UV-Vis absorption and (B), (D) normalized PL of the pyreno[2,1-b]furan molecules **2** and **3** in THF (10  $\mu$ M) and in the solid state at room temperature. Insert: fluorescent photographs of **2** and **3** taken under 365 nm UV irradiation in THF solution and in the solid state, respectively.

**Table 1.** Physical and Electrochemical Properties of pyreno[2,1-b]furan molecules **2** and **3**.

Comd.	$\lambda_{\text{abs}}$ (nm)	$\lambda_{\text{maxPL}}$ (nm)	Stock shift (nm)	$\Phi_f$	$\tau$ (ns)	LUMO (eV) <sup>b</sup>	HOMO (eV) <sup>b</sup>	$E_g$ (eV) <sup>b</sup>
<b>2a</b>	348, 495 <sup>a</sup>	516, 550 <sup>a</sup>	21 <sup>a</sup>	0.839 <sup>a</sup>	2.68 <sup>a</sup>	-2.33	-4.76	2.43
	373, 540 <sup>b</sup>	636 <sup>b</sup>	96 <sup>b</sup>	0.155 <sup>b</sup>	7.75 <sup>b</sup>			
<b>2b</b>	342, 489	510, 543	21	0.851	2.61	-2.49	-4.95	2.46
	344, 470	625	155	0.266	16.97			
<b>2c</b>	342, 488	508, 540	20	0.777	2.64	-3.20	-5.64	2.44
	341, 464	639	175	0.157	18.86			
<b>3</b>	338, 484	505, 536	21	0.791	2.72	-2.56	-5.05	2.50
	355, 472	640	168	0.028	6.68			

<sup>a</sup>) Absorption wavelength measured in THF solution at room temperature. <sup>b</sup>) in thin film. <sup>c</sup>) DFT (B3LYP/6-311G (d,p)) calculations.

Upon excitation, all compounds emit intense green emission with maximum emission peaks at 516 nm for **2a**, 510 nm for **2b**, 508 nm for **2c** and 505 nm for **3** (Figure 1B), respectively, with high fluorescence quantum yields ( $\Phi_f$ ) in the range 0.78-0.85 in THF solution, in the order *tert*-butyl (**2b**) > methoxyl (**2a**) > thiophenyl (**3**) > trifluoromethyl (**2c**). In addition, compound **2a** exhibits a red shifted emission of 20 nm compared with 1,3,6,8-tetrakis(4-methoxy-phenylethynyl)pyrene.<sup>22</sup> On the other hand, all compounds in the solid state are orange-red in color with a broaden absorption band from 320-800 nm. The maximum long wavelength absorption exhibited by **2a** is red shifted to 540 nm. The pyreno[2,1-b]furan molecules exhibit a blue shifted absorption peak at 489 nm for **2b**, 488 nm for **2c** and 472 nm for **3**, respectively. The former originate from the J-aggregation and the latter may be attributed to the formation of H-aggregation,<sup>33</sup> which is consistent with the crystal packing pattern. The maximum photoluminescence (PL) peaks of compounds **2** and **3** were recorded in the range 625-640 nm, and a large red shifted emission (~82 nm) was observed for these compounds in the film state compared to in THF solution. This is due to the expanded  $\pi$ -conjugated molecular structures, resulting in stronger  $\pi$ - $\pi$  stacking interactions in the solid state, and  $\Phi_f$  decreased to 0.03-0.27. The concentration-dependent PL spectra for compounds **2** and **3** were also measured. Taking compound **2a** as example, it exhibits a maximum emission peak at 514 nm with a shoulder peak at 550 nm over the concentration range  $10^{-7}$  to  $10^{-5}$  M. As the concentration increased from  $10^{-4}$  to  $10^{-3}$  M, the shoulder emission peak at 550 nm was enhanced with a fading emission peak at 514 nm. We infer that the emission peak at 550 nm is originating from different vibrational

progression.<sup>34</sup> Also, the compounds **2b**, **2c** and **3** show a similar concentration-dependent PL behavior (Figure S27). Moreover, as the concentration increased, the proton peaks of the pyreno[2,1-b]furan framework and the phenyl ring were shifted upfield according to their <sup>1</sup>H NMR spectra, indicated that compounds **2** and **3** exhibit strong  $\pi$ - $\pi$  stacking interactions (Figures S9-S12).

### 2.3 DFT calculations

Furthermore, the optimized geometric conformation and electron distributions were investigated at the 6-311G(d,p) basis set using Gaussian 09 program by DFT calculations. The optimized geometries revealed that the pyreno[2,1-b]furan molecules arrange with near co-planar conformations, with a twist angle less than 2°, which is beneficial to forming  $\pi$ ··· $\pi$  stacking in the aggregated state, which is consistent with the optical properties. Compared to alkynylpyrene derivatives,<sup>24,35</sup> the highest occupied molecular orbitals (HOMO) and the lowest unoccupied molecular orbitals (LUMO) were both mainly located on the pyreno[2,1-b]furan core, the furan ring and a fragment of the substituent groups (Figure 2). The solvatochromic effect indicated that both UV-vis absorption and PL spectra of compound **2** show a positive solvatochromism with a red shifted absorption band of ~15 nm and the emission was red shifted by 17~20 nm along with a successive decreased in fluorescence intensity (Figures S23-S26). This studies indicated that the slightly separated HOMO and LUMO lead to solvent dependent red shifted emission, which is due to the

synergetic effect of intramolecular charge transfer (ICT) and local excited state under irradiation.<sup>36</sup>

According to the DFT calculations, although compounds **2** have a similar energy gap, **2c** illustrated higher HOMO and LUMO levels compared to **2a** and **2b**, and **3**, which may contribute to the easier hole injection and strength of the hole transport ability.<sup>37,38</sup>

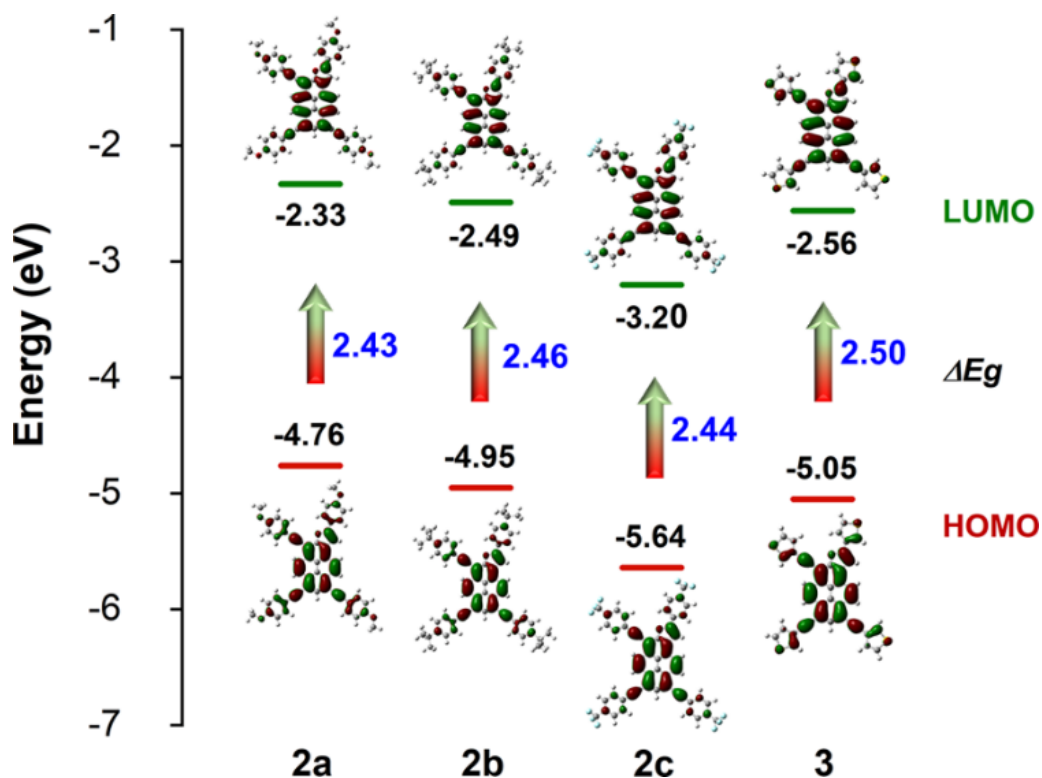


**Figure 2.** Molecular orbital plots of **2** and **3** calculated at the B3LYP/6-311G(d,p) level.

## 2.4 Two-photon absorption properties

Inspired by the two-photon absorption properties of 1,3,6,8-alkynyl-conjugated pyrenes,<sup>6</sup> two-photon excitation fluorescence spectra of the pyreno[2,1-b]furan molecules **2**, were performed in DMSO (5  $\mu$ M). The emission signals were collected under different pulse wavelength (740-880 nm) excitation. As shown in Figure S30, three compounds **2a-2c**

exhibit intense two-photon excitation fluorescence in the range 740-880 nm. Using rhodamine B as the standard, the calculated two-photon absorption cross section ( $\delta$ ) are presented in Figure 3A, and the maximum  $\delta$  is 438 GM for **2a**, 533 GM for **2b** and 234 GM for **2c**, under laser excitation at 800 nm, respectively. The results indicated that although the compounds possess the same pyreno[2,1-b]furan skeleton and  $\pi$ -conjugated chain length, the electron donating groups at the terminus play a significant role in improving the TPA cross section in the pyrene system. Moreover, the fluorescence intensity enhanced relatively linearly as the laser power increased, and the log-log plot of the fluorescence integral *versus* pumped power were fitted linearly with slope of 1.86 for **2a**, 1.81 for **2b** and 1.78 for **2c**, respectively, indicating a facile two-photon excitation mechanism for the pyreno[2,1-b]furan molecules **2** (Figures 3C). Thus, the excellent PL properties with a high  $\delta$  value of **2** would make an impressive two-photon fluorescent material for potential application in bioimaging.

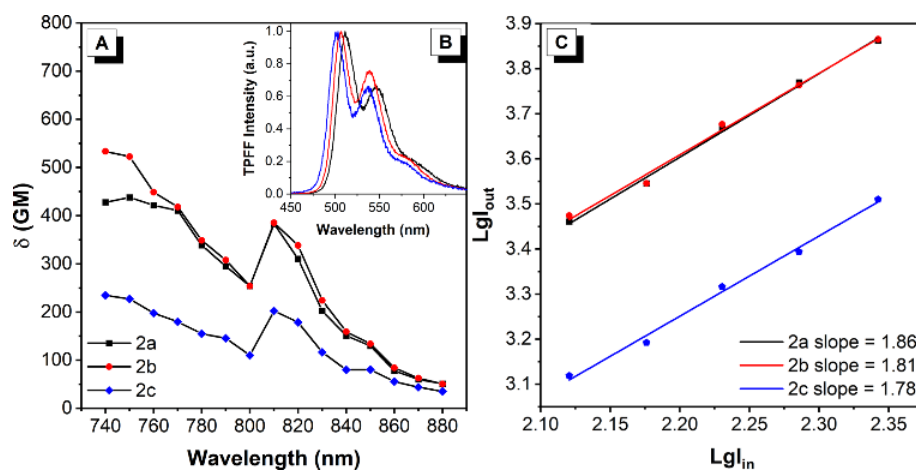


**Figure 3.** (A) Two-photon action cross-section; (B) Normalized two-photon excited fluorescence of **2** in DMSO solution (5  $\mu$ M) under 740 nm excitation; (C) the log-log plot of

the fluorescence integral ( $I_{\text{out}}$ ) *versus* pumped power ( $I_{\text{in}}$ ) and at different excitation intensities (mW) irradiated by an 800 nm femtosecond pulsed laser light.

### **3. Conclusions**

In summary, we report a facile, one-pot synthesis of pyreno[2,1-b]furan molecules from a new bromopyrene intermediate. The molecular structures were fully characterized. The new pyreno[2,1-b]furan molecules with expanded  $\pi$ -conjugated molecular skeletons display differentiable emission behavior both in solution and in the solid state, which can be attributed to the planar structure, leading to  $\pi$ - $\pi$  stacking. These preliminary results indicated that the pyreno[2,1-b]furan molecules are excellent TPA fluorophores with a  $\delta$  value of 533 GM in DMSO, and the terminal group with electron donating properties plays a significant role in regulating the  $\delta$  value. Thus, this study not only offers a synthetic method to new pyreno[2,1-b]furan molecules and is beneficial for expanding the applications of such molecules not only in organic electronics, but also would be as great nonlinear optical materials yield for potential application in bioimaging. Further research on the applications of such molecules is ongoing in our laboratory.

## **4. Experimental**

### **4.1 Materials**

Unless otherwise stated, all reagents used were purchased from commercial sources and were used without further purification. Specpure grade solvents were used for spectroscopic

measurements. The pyrene-based intermediate 1,3,6,8-tetrabromo-2-hydroxypyrene (**1**) was synthesized following the reported procedure.<sup>23</sup>

## 4.2 Characterization

<sup>1</sup>H and <sup>13</sup>C NMR spectra were recorded on a Bruker AV 400M spectrometer using chloroform-*d* solvent and THF-*d*8 and tetramethylsilane as internal reference. *J*-values are given in Hz. <sup>1</sup>H NMR and <sup>1</sup>H-<sup>1</sup>H NOSEY NMR spectroscopy were recorded on a Bruker AV 600M using chloroform-*d* solvent and THF-*d*8 solvent. High-resolution mass spectra (HRMS) were recorded on a LC/MS/MS, which consisted of a HPLC system (Ultimate 3000 RSLC, Thermo Scientific, USA) and a Q Exactive Orbitrap mass spectrometer. UV-vis absorption spectra and photoluminescence (PL) spectra were recorded on a Shimadzu UV-2600 and the Hitachi F-4700 spectrofluorometer. PL quantum yields were measured using absolute methods using a Hamamatsu C11347-11 Quantaaurus-QY Analyzer. The fluorescence lifetime was recorded on an Edinburgh FLS 980 instrument and measured using a time-correlated single-photon counting method. Thermogravimetric analysis was carried on a Mettler Toledo TGA/DSC3+ under dry nitrogen at a heating rate of 10 °C/min. The quantum chemistry calculations were performed using the Gaussian 09 (B3LYP/6-311G (d,p) basis set) software package. [Structural assignments were made with additional information from gCOSY experiments.](#)

## 4.3 X-ray Crystallography

Crystallographic data for **2b** was collected on a Bruker APEX 2 CCD diffractometer with graphite monochromated Mo K $\alpha$  radiation ( $\lambda = 0.71073 \text{ \AA}$ ) in the  $\omega$  scan mode.<sup>33 34</sup> The



structure was solved by charge flipping algorithms and refined by full-matrix least-squares methods on  $F^2$ .<sup>39 40</sup> All esds (except the esd in the dihedral angle between two l.s. planes) were estimated using the full covariance matrix. The cell esds were considered individually in the estimation of esds in distances, angles and torsion angles. Correlations between esds in cell parameters were only used when they were defined by crystal symmetry. An approximate (isotropic) treatment of cell esds was used for estimating esds involving l.s. planes. The final cell constants were determined through global refinement of the xyz centroids of the reflections harvested from the entire data set. Structure solution and refinements were carried out using the SHELXTL-PLUS software package.<sup>39</sup> Data (excluding structure factors) on the structure reported here has been deposited with the Cambridge Crystallographic Data Centre. CCDC 2166623 for **2b** contains the supplementary crystallographic data for this paper. These data could be obtained free of charge from The Cambridge Crystallographic Data Centre via [www.ccdc.cam.ac.uk/data\\_request/cif](http://www.ccdc.cam.ac.uk/data_request/cif).

#### 4.4 Synthetic procedures

##### Synthesis of 2-hydroxypyrene (Py-OH).<sup>41</sup>

Under a nitrogen atmosphere, a mixture of pyrene-2-(4,4,5,5-tetramethyl-[1,3,2]dioxaborolane)<sup>42</sup> (600 mg, 1.8 mmol, 1.0 eq.) and NaOH (270 mg, 4.6 mmol, 2.5 eq.) in THF (70 mL) was stirred for 10 min. Then, an aqueous solution of H<sub>2</sub>O<sub>2</sub> (0.5 mL, 30%) and 1 mL H<sub>2</sub>O was added into the mixture and stirred for 4 h at room temperature, and then the solution was acidified to pH 1–2 by using 1 M HCl. The product was

evaporated and extracted with dichloromethane (3 × 30 mL) three times, washed with saturated brine (50 mL), and dried with MgSO<sub>4</sub>. The organic phase was evaporated and the residue was dissolved in 3 mL ethyl acetate. Then, ethanol (200 mL) was added until the precipitate appeared, which was further filtered under reduced pressure to afford compound **Py-OH** as a light-green solid (360 mg, 91% yield). <sup>1</sup>H NMR (400 MHz, CDCl<sub>3</sub>): δ 8.16 (d, J = 7.6 Hz, 2H), 8.06 (d, J = 9.0 Hz, 2H), 7.98 – 7.90 (m, 3H), 7.64 (s, 2H), 5.45 (s, 1H, OH) ppm, which is consistent with Marder's report.<sup>34,41</sup>

### **Synthesis of 1,3,6,8-tetrabromo-2-hydroxypyrene (1)**<sup>23</sup>

A mixture of bromine (0.65 mL, 12.0 mmol, 6 eq.) with nitrobenzene (10 mL) was added dropwise to a solution of **Py-OH** (516 mg, 2.0 mmol, 1 eq.) in nitrobenzene (40 mL). The mixture was vigorously stirred at 120°C for 24 h. After cooling to room temperature, a brown precipitate formed. The mixture was filtered with hexane (200 mL) under reduced pressure to afford compound **1** as a bright-brown solid (941 mg, yield at 89%) (melting point: > 300°C), which was insoluble in common organic solvents, such as chloroform and DMSO, but slightly soluble in ethanol. The product was not further purified and was used as such for the Suzuki coupling reactions directly. The solid was characterized by HRMS. HRMS (FTMS - p APCI) m/z: [M - H]<sup>-</sup> Calcd for C<sub>16</sub>H<sub>5</sub>Br<sub>4</sub>O 532.8268; Found, 532.7036.

**Synthesis of 8-(4-methoxyphenyl)-1,3,6-tris((4-methoxyphenyl)ethynyl)pyreno[2,1-b]furan (2a).**

The pyreno[2,1-b]furans **2** and **3** were synthesized from 1,3,6,8-tetrabromo-2,7-dihydroxypyrene (**1**) using the corresponding arylboronic acid by a Sonogashira reaction in considerable yield.<sup>43</sup>

A mixture of **1** (320 mg, 0.6 mmol, 1.0 eq.), 1-ethynyl-4-methoxybenzene (475 mg, 3.6 mmol, 6.0 eq.) and CuI (100 mg, 0.5 mmol, 0.9 eq.) were dissolved in DMF (5 mL) and Et<sub>3</sub>N (5 mL) and stirred under a nitrogen atmosphere, then PdCl<sub>2</sub>(PPh<sub>3</sub>)<sub>2</sub> (50 mg, 0.07 mmol, 0.1 eq.) was added, and the mixture was vigorously stirred at 90°C for 48 h. After cooling to room temperature, the reaction mixture was quenched with water (50 mL) and extracted with ethyl acetate three times (3 × 30 mL). The combined organic layer was washed with water and brine (100 mL), dried over MgSO<sub>4</sub> and evaporated. The crude product was further purified by column chromatography with hexane/ chloroform (V<sub>hexane</sub>: V<sub>CHCl<sub>2</sub></sub> = 2:1) as the eluent to afford 8-(4-methoxyphenyl)-1,3,6-tris((4-methoxyphenyl)ethynyl)pyreno[2,1-b]furan (**2a**) as an orange-red solid (120 mg, 27%. Due to the low solubility, the target compound **2a** was adsorbed by silica gel in the purification process, leading to a low yield.), which was recrystallization (V<sub>hexane</sub>: V<sub>CHCl<sub>3</sub></sub> = 1:2) to afford **2a** as an orange-red solid. Melting point: 188-190 °C <sup>1</sup>H NMR (400 MHz, CDCl<sub>3</sub>) δ 8.73 (d, *J* = 9.2 Hz, 1H), 8.67 (d, *J* = 8.9 Hz, 1H), 8.60 (d, *J* = 9.2 Hz, 1H), 8.37 (d, *J* = 9.0 Hz, 1H), 8.31 (s, 1H), 8.01 (d, *J* = 8.7 Hz, 2H), 7.77 (d, *J* = 8.7 Hz, 2H), 7.77 (d, *J* = 8.7 Hz, 2H), 7.67 (d, *J* = 2.1 Hz, 2H), 7.65 (d, *J* = 2.2 Hz, 2H), 7.57 (s, 1H), 7.05 (d, *J* = 8.8 Hz, 2H), 7.01 (d, *J* = 8.7 Hz, 2H), 6.97 (d, *J* = 8.2 Hz, 4H), 3.91 (s, 6H), 3.89 (s, 6H) ppm. <sup>13</sup>C {<sup>1</sup>H} NMR (100 MHz, CDCl<sub>3</sub>) δ 160.7, 160.4, 160.2, 157.9, 152.5, 133.2, 133.0, 132.1, 130.8,

129.1, 126.6, 125.8, 125.6, 124.8, 124.7, 124.2, 123.7, 122.8, 120.9, 118.2, 118.2, 115.5, 115.4, 114.2, 114.1, 114.0, 103.1, 100.5, 98.8, 95.8, 95.6, 86.6, 86.6, 81.6, 54.7, 54.6, 29.7 ppm. HRMS (FTMS + p APCI) m/z: [M+H]<sup>+</sup> Calcd for C<sub>52</sub>H<sub>35</sub>O<sub>5</sub> 739.2479; Found, 739.2479.

**Synthesis of 8-(4-(*tert*-butyl)phenyl)-1,3,6-tris((4-(*tert*-butyl)phenyl)ethynyl)pyreno[2,1-b]furan (2b).**

8-(4-(*tert*-butyl)phenyl)-1,3,6-tris((4-(*tert*-butyl)phenyl)ethynyl)pyreno[2,1-b]furan (**2b**) was purified by column chromatography using hexane as the eluent to afford **2b** as an orange-red solid (100 mg, 59%). <sup>1</sup>H NMR (400 MHz, CDCl<sub>3</sub>) δ 8.71 (d, *J* = 9.2 Hz, 1H), 8.64 (d, *J* = 9.0 Hz, 1H), 8.59 (d, *J* = 9.2 Hz, 1H), 8.34 (d, *J* = 9.0 Hz, 1H), 8.31 (s, 1H), 8.00 (d, *J* = 8.4 Hz, 2H), 7.78 (d, *J* = 8.3 Hz, 2H), 7.69 (d, *J* = 2.4 Hz, 2H), 7.67 (d, *J* = 2.4 Hz, 2H), 7.63 (s, 1H), 7.55 (d, *J* = 8.4 Hz, 2H), 7.51 (d, *J* = 8.4 Hz, 2H), 7.48 (d, *J* = 1.0 Hz, 2H), 7.45 (d, *J* = 1.2 Hz, 2H), 1.42 (s, 18H), 1.39 (s, 18H) ppm. <sup>13</sup>C {<sup>1</sup>H} NMR (100 MHz, CDCl<sub>3</sub>) δ 157.7, 152.8, 152.2, 151.9, 151.7, 151.7, 132.6, 131.7, 131.6, 131.3, 131.1, 129.5, 127.4, 126.9, 125.9, 125.8, 125.5, 125.5, 125.3, 125.2, 125.1, 124.7, 124.2, 123.9, 120.9, 120.7, 120.6, 118.0, 103.1, 100.5, 99.7, 95.8, 95.6, 87.8, 87.7, 82.7, 68.0, 50.9, 35.0, 34.9, 31.6, 31.3, 31.3, 31.3 ppm. HRMS (FTMS - p APCI) m/z: [M-H]<sup>-</sup> Calcd for C<sub>64</sub>H<sub>57</sub>O 842.4493; Found, 842.4502.

**Synthesis of 8-(4-(trifluoromethyl)phenyl)-1,3,6-tris((4-(trifluoromethyl)phenyl)ethynyl)pyreno[2,1-b]furan (2c).**

The compound 8-(4-(trifluoromethyl)phenyl)-1,3,6-tris((4-(trifluoromethyl)phenyl)ethynyl)pyreno [2,1-b] furan (**2c**) was purified by column chromatography using dichloromethane as the eluent to afford **2c** as an orange-red solid (80 mg, 22%) **Melting point: 117-119 °C**. <sup>1</sup>H NMR (400 MHz, [D<sub>8</sub>]-THF) δ 8.78 (d, *J* = 4.9 Hz, 1H), 8.75 (d, *J* = 4.6 Hz, 1H), 8.65 (d, *J* = 9.3 Hz, 1H), 8.62 (d, *J* = 9.0 Hz, 1H), 8.41 (s, 1H), 8.30 (d, *J* = 6.4 Hz, 3H), 8.02 (d, *J* = 7.9 Hz, 2H), 7.90 (d, *J* = 5.8 Hz, 4H), 7.85 (d, *J* = 8.6 Hz, 2H), 7.82 (d, *J* = 8.5 Hz, 2H), 7.78 (d, *J* = 7.9 Hz, 4H) ppm. The <sup>13</sup>C NMR spectrum of this compound could not be determined due to its low solubility. HRMS (FTMS - p APCI) *m/z*: [M-H]<sup>-</sup> Calcd for C<sub>52</sub>H<sub>21</sub>F<sub>12</sub>O 890.1485; Found, 890.1493.

### **Synthesis of 8-(thiophen-3-yl)-1,3,6-tris(thiophen-3-ylethynyl)pyreno[2,1-b]furan (3).**

The 8-(thiophen-3-yl)-1,3,6-tris(thiophen-3-ylethynyl)pyreno[2,1-b]furan (**3**) was purified by column chromatography using dichloromethane as the eluent to afford **3** as an orange-red solid (40 mg, 16%) **Melting point: 166-168 °C**. Due to the low solubility, the target compound **3** was adsorbed by silica gel during the purification process, leading to a low yield. <sup>1</sup>H NMR (400 MHz, [D<sub>8</sub>]-THF) δ 8.79 (d, *J* = 9.2 Hz, 1H), 8.74 (d, *J* = 9.0 Hz, 1H), 8.65 (d, *J* = 9.2 Hz, 1H), 8.58 (d, *J* = 9.0 Hz, 1H), 8.32 (s, 1H), 8.14 (dd, *J* = 2.9, 1.1 Hz, 1H), 7.99 (dd, *J* = 2.9, 1.1 Hz, 1H), 7.90 (s, 1H), 7.87 (td, *J* = 2.9, 1.1 Hz, 2H), 7.75 (dd, *J* = 5.0, 1.1 Hz, 1H), 7.62 (dd, *J* = 5.0, 2.9 Hz, 1H), 7.58 (dd, *J* = 4.9, 3.0 Hz, 1H), 7.56 – 7.52 (m, 2H), 7.50 (dd, *J* = 4.9, 1.1 Hz, 1H), 7.40 (d, *J* = 5.0 Hz, 2H) ppm. The <sup>13</sup>C NMR spectrum of this compound could not be determined due to its low solubility. HRMS (FTMS - p APCI) *m/z*: [M-H]<sup>-</sup> Calcd for C<sub>40</sub>H<sub>17</sub>OS<sub>4</sub> 642.0246; Found, 642.0253.

### **Synthesis of 2-(4-methoxyphenyl)benzofuran (MBF).**

A mixture of 2-bromophenol (350 mg, 2 mmol, 1.0 eq.), 3-ethynylthiophene (260 mg, 2 mmol, 6.0 eq.), PPh<sub>3</sub> (100 mg, 0.4 mmol, 0.19 e.q.) and CuI (100 mg, 0.5 mol, 0.3 eq.) were dissolved in DMF (5 mL) and Et<sub>3</sub>N (5 mL) and stirred under a nitrogen atmosphere, and then PdCl<sub>2</sub>(PPh<sub>3</sub>)<sub>2</sub> (106 mg, 0.15 mmol, 0.08 eq.) was added and the mixture was vigorously stirred at 120°C for 48 h. After cooling to room temperature, the reaction mixture was quenched with water (50 mL), and extracted with DCM three times (3 × 30 mL). The combined organic layer was washed with water and brine (100 mL), then dried over MgSO<sub>4</sub> and evaporated. The crude product was further purified by column chromatography using hexane/dichloromethane (V<sub>hexane</sub>: V<sub>CH<sub>2</sub>Cl<sub>2</sub></sub> = 2:1) as the eluent to afford 2-(4-methoxyphenyl)benzofuran (**MBF**) as a white solid (50 mg, 11%). <sup>1</sup>H NMR (400 MHz, CDCl<sub>3</sub>) δ 7.80 (d, J = 8.8 Hz, 2H), 7.55 (d, J = 4 Hz, 1H), 7.50 (d, J = 7.9 Hz, 1H), 7.22 (dt, J = 7.3, 4.1 Hz, 2H), 6.98 (d, J = 8.8 Hz, 2H), 6.89 (s, 1H) ppm, which is consistent with Ollivier's report.<sup>44</sup>

**4.5. Preparation of the film:** The pyreno[2,1-b]furan molecules (5 mg) were dissolved in THF (10 mL) and spin-coated in silicon pellet at 500 rp/min at room temperature. The prepared thin film was utilized for fluorescence measurements.

### **ASSOCIATED CONTENT**

#### **Supporting Information**

The Supporting Information is available free of charge on the ACS Publications website.

Details of the experimental characterization, including  $^1\text{H}/^{13}\text{C}$  NMR spectra, HRMS. Results of UV-vis and fluorescence spectra, crystal parameters, Two-photon excited fluorescent spectra and DFT calculations (PDF).

Single crystal X-ray diffraction of **2b** (CIF)

## AUTHOR INFORMATION

### Corresponding Author

**Xing Feng** - Guangdong Provincial Key Laboratory of Information Photonics Technology, School of Material and Energy, Guangdong University of Technology, Guangzhou 510006, P. R. China, [orcid.org/0000-0002-4273-979X](https://orcid.org/0000-0002-4273-979X); E-mail: [hyxhn@sina.com](mailto:hyxhn@sina.com).

**Guangle Niu** - Center of Bio and Micro/Nano Functional Materials, State Key Laboratory of Crystal Materials, Shandong University, Jinan 250100, P. R. China. Email: [niugl@sdu.edu.cn](mailto:niugl@sdu.edu.cn) (G. Niu)

### Authors

**Xiaohui Wang** - Guangdong Provincial Key Laboratory of Information Photonics Technology, School of Material and Energy, Guangdong University of Technology, Guangzhou 510006, P. R. China. [orcid.org/0000-0001-7506-2845](https://orcid.org/0000-0001-7506-2845)

**Chengjing Zhang** - Center of Bio and Micro/Nano Functional Materials, State Key Laboratory of Crystal Materials, Shandong University, Jinan 250100, P. R. China.

**Xiaoyu Mao** - Guangdong Provincial Key Laboratory of Functional Soft Condensed Matter, School of Material and Energy, Guangdong University of Technology, Guangzhou 510006, P. R. China

**Carl Redshaw** - Department of Chemistry, University of Hull, Cottingham Road, Hull, Yorkshire HU6 7RX, UK.

**Xiaoqiang Yu** - Center of Bio and Micro/Nano Functional Materials, State Key Laboratory of Crystal Materials, Shandong University, Jinan 250100, P. R. China.

### **Author Contributions**

#X. W. and C. Z. contributed equally to this paper.

### **Notes**

The authors declare no competing financial interest.

### **ACKNOWLEDGMENT**

§J.S. and M.W. contributed equally to this paper. This work was supported by the National Natural Science Foundation of China (21975054), Natural Science Foundation of Guangdong Province of China (2019A1515010925), Guangdong Provincial Key Laboratory of Information Photonics Technology (2020B121201011), “One Hundred Talents Program” of the Guangdong University of Technology (GDUT) (1108-220413205), the Open Fund of Guangdong Provincial Key Laboratory of Luminescence from Molecular Aggregates, Guangzhou 510640, China (South China University of Technology) (2019B030301003), Science and Technology Planning Project of Hunan Province (2018TP1017), CR thanks the University of Hull for support.

### **References**

- (1) Yang, Z.; Mao, Z.; Xie, Z.; Zhang, Y.; Liu, S.; Zhao, J.; Xu, J.; Chi, Z.; Aldred, M. P. Recent Advances in Organic Thermally Activated Delayed Fluorescence Materials. *Chem. Soc. Rev.* 2017, 46, 915-1016.



- (2) Dimitriev, O. P. Dynamics of Excitons in Conjugated Molecules and Organic Semiconductor Systems. *Chem. Rev.* 2022, 122, 8487–8593.
- (3) Yang, Y.; Zhao, Q.; Feng, W.; Li, F. Luminescent Chemodosimeters for Bioimaging. *Chem. Rev.* 2013, 113, 192-270.
- (4) Liu, Y.; Li, Y.; Koo, S.; Sun, Y.; Liu, Y.; Liu, X.; Pan, Y.; Zhang, Z.; Du, M.; Lu, S.; Qiao, X.; Gao, J.; Wang, X.; Deng, Z.; Meng, X.; Xiao, Y.; Kim, J. S.; Hong, X. Versatile Types of Inorganic/Organic NIR-IIa/IIb Fluorophores: From Strategic Design toward Molecular Imaging and Theranostics. *Chem. Rev.* 2022, 122, 209-268.
- (5) Li, Y.; Tang, R.; Liu, X.; Gong, J.; Zhao, Z.; Sheng, Z.; Zhang, J.; Li, X.; Niu, G.; Kwok, R. T. K.; Zheng, W.; Jiang, X.; Tang, B. Z. Bright Aggregation-Induced Emission Nanoparticles for Two-Photon Imaging and Localized Compound Therapy of Cancers. *ACS Nano* 2020, 14, 16840-16853.
- (6) Kim, H. M.; Lee, Y. O.; Lim, C. S.; Kim, J. S.; Cho, B. R. Two-photon Absorption Properties of Alkynyl-Conjugated Pyrene Derivatives. *J. Org. Chem.* 2008, 73, 5127-5130.
- (7) Figueira-Duarte, T. M.; Mullen, K. Pyrene-based Materials for Organic Electronics. *Chem. Rev.* 2011, 111, 7260-7314.
- (8) Islam, M. M.; Hu, Z.; Wang, Q.; Redshaw, C.; Feng, X. Pyrene-Based Aggregation-Induced Emission Luminogens and their Applications. *Mater. Chem. Front.* 2019, 3, 762-781.
- (9) Wu, Z. H.; Huang, Z. T.; Guo, R. X.; Sun, C. L.; Chen, L. C.; Sun, B.; Shi, Z. F.; Shao, X.; Li, H.; Zhang, H. L. 4,5,9,10-Pyrene Diimides: A Family of Aromatic Diimides Exhibiting High Electron Mobility and Two-Photon Excited Emission. *Angew. Chem. Int. Ed.* 2017, 56, 13031--13035.
- (10) Feng, X.; Xu, Z.; Hu, Z.; Qi, C.; Luo, D.; Zhao, X.; Mu, Z.; Redshaw, C.; Lam, J. W. Y.; Ma, D.; Tang, B. Z. Pyrene-Based Blue Emitters with Aggregation-Induced Emission Features for High-Performance Organic Light-Emitting Diodes. *J. Mater. Chem. C* 2019, 7, 2283-2290.
- (11) Zophel, L.; Enkelmann, V.; Mullen, K. Tuning the HOMO-LUMO Gap of Pyrene Effectively via Donor-Acceptor Substitution: Positions 4,5 versus 9,10. *Org. Lett.* 2013, 15, 804-807.
- (12) Feng, X.; Tomiyasu, H.; Hu, J. Y.; Wei, X.; Redshaw, C.; Elsegood, M. R.; Horsburgh, L.;

- Teat, S. J.; Yamato, T. Regioselective Substitution at the 1,3- and 6,8-Positions of Pyrene for the Construction of Small Dipolar Molecules. *J. Org. Chem.* 2015, 80, 10973-10978.
- (13) Wang, C.-Z.; Zhang, R.; Sakaguchi, K.; Feng, X.; Yu, X.; Elsegood, M. R. J.; Teat, S. J.; Redshaw, C.; Yamato, T. Two-Photon-Absorption Properties of Pyrene-Based Dipolar D- $\pi$ -A Fluorophores. *ChemPhotoChem* 2018, 2, 749-756.
- (14) Sonar, P.; Soh, M. S.; Cheng, Y. H.; Henssler, J. T.; Sellinger, A. 1,3,6,8-tetrasubstituted Pyrenes: Solution-Processable Materials for Application in Organic Electronics. *Org. Lett.* 2010, 12, 3292-3295.
- (15) Zhang, S.; Liu, Z.; Fang, Q. Synthesis, Structures, and Optoelectronic Properties of Pyrene-Fused Thioxanthenes. *Org. Lett.* 2017, 19, 1382-1385.
- (16) Min, Y.; Dou, C.; Tian, H.; Geng, Y.; Liu, J.; Wang, L. n-Type Azaacenes Containing B $\leftarrow$ -N Units. *Angew. Chem. Int. Ed.* 2018, 57, 2000 -2004.
- (17) Min, Y.; Dou, C.; Liu, D.; Dong, H.; Liu, J. Quadruply B $\leftarrow$ -N-Fused Dibenzo-Azaacene with High Electron Affinity and High Electron Mobility. *J. Am. Chem. Soc.* 2019, 141, 17015-17021.
- (18) Kojima, T.; Yokota, R.; Kitamura, C.; Kurata, H.; Tanaka, M.; Ikeda, H.; Kawase, T. Pyreno[4,5-b]furan and Pyreno[4,5-b:9,10-b']difuran Derivatives as New Blue Fluorophores: Synthesis, Structure, and Electronic Properties. *Chem. Lett.* 2014, 43, 696-698.
- (19) Xiao, J.; Yang, B.; Wong, J. I.; Liu, Y.; Wei, F.; Tan, K. J.; Teng, X.; Wu, Y.; Huang, L.; Kloc, C.; Boey, F.; Ma, J.; Zhang, H.; Yang, H. Y.; Zhang, Q. Synthesis, Characterization, Self-Assembly, and Physical Properties of 11-methylbenzo[d]pyreno[4,5-b]furan. *Org. Lett.* 2011, 13, 3004-3007.
- (20) Wang, S.; Lv, B.; Cui, Q.; Ma, X.; Ba, X.; Xiao, J. Synthesis, Photophysics, and Self-Assembly of Furan-Embedded Heteroarenes. *Chem. Eur. J.* 2015, 21, 14791-14796.
- (21) Baumgartner, K.; Kirschbaum, T.; Krutzek, F.; Dreuw, A.; Rominger, F.; Mastalerz, M. K-Region-Extended [c]-Heteroannulated Pyrenes. *Chem. Eur. J.* 2017, 23, 17817-17822.
- (22) Hu, J.-y.; Era, M.; Elsegood, M. R. J.; Yamato, T. Synthesis and Photophysical Properties of Pyrene-Based Light-Emitting Monomers: Highly Pure-Blue-Fluorescent, Cruciform-Shaped

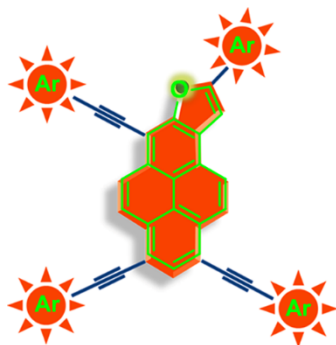
- Architectures. *Eur. J. Org. Chem.* 2010, 2010, 72-79..
- (23) Wang, X.; Zhang, J.; Mao, X.; Liu, Y.; Li, R.; Bai, J.; Zhang, J.; Redshaw, C.; Feng, X.; Tang, B. Z. Intermolecular Hydrogen-Bond-Assisted Solid-State Dual-Emission Molecules with Mechanical Force-Induced Enhanced Emission. *J. Org. Chem.* 2022, 87, 8503-8514.
- (24) Oh, J.-W.; Lee, Y. O.; Kim, T. H.; Ko, K. C.; Lee, J. Y.; Kim, H.; Kim, J. S. Enhancement of Electrogenerated Chemiluminescence and Radical Stability by Peripheral Multidonors on Alkynylpyrene Derivatives. *Angew. Chem.* 2009, 121, 2560-2562.
- (25) Ghosh, S.; Das, J.; Saikh, F. A New Synthesis of 2-aryl/alkylbenzofurans by Visible Light Stimulated Intermolecular Sonogashira Coupling and Cyclization Reaction in Water. *Tetrahedron Lett.* 2012, 53, 5883-5886.
- (26) Bhadra, M.; Sasmal, H. S.; Basu, A.; Midya, S. P.; Kandambeth, S.; Pachfule, P.; Balaraman, E.; Banerjee, R. Predesigned Metal-Anchored Building Block for In Situ Generation of Pd Nanoparticles in Porous Covalent Organic Framework: Application in Heterogeneous Tandem Catalysis. *ACS Appl. Mater. Interfaces* 2017, 9, 13785-13792.
- (27) Biffis, A.; Centomo, P.; Del Zotto, A.; Zecca, M. Pd Metal Catalysts for Cross-Couplings and Related Reactions in the 21st Century: A Critical Review. *Chem. Rev.* 2018, 118, 2249-2295.
- (28) Martinez, C.; Alvarez, R.; Aurrecoechea, J. M. Palladium-catalyzed Sequential Oxidative Cyclization/Coupling of 2-alkynylphenols and Alkenes: a Direct Entry into 3-Alkenylbenzofurans. *Org. Lett.* 2009, 11, 1083-1086.
- (29) Isono, N.; Lautens, M. Rhodium(I)-Catalyzed Cyclization Reaction of o-Alkynyl Phenols and Anilines. Domino Approach to 2,3-Disubstituted Benzofurans and Indoles. *Org. Lett.* 2009, 11, 1329-1331.
- (30) Fukazawa, A.; Yamada, H.; Sasaki, Y.; Akiyama, S.; Yamaguchi, S. Zwitterionic Ladder Bis(arylethenyl)benzenes with Large Two-Photon Absorption Cross Sections. *Chem. Asian. J.* 2010, 5, 466-469.
- (31) Akther, T.; Islam, M. M.; Matsumoto, T.; Tanaka, J.; Feng, X.; Redshaw, C.; Yamato, T. Demethylation of 5,n-di-tert-butyl-8,n-dimethoxy[2.n]metacyclophane-1-yne with BBr<sub>3</sub> to Afford Novel [n]benzofuranophanes. *J. Mol. Struct.* 2016, 1122, 247-255.

- (32) Zhou, R.; Wang, W.; Jiang, Z. J.; Wang, K.; Zheng, X. L.; Fu, H. Y.; Chen, H.; Li, R. X. One-Pot Synthesis of 2-Substituted benzo[b]furans via Pd-tetrakisphosphine Catalyzed Coupling of 2-halophenols with Alkynes Chem. Commun. 2014, 50, 6023-6026.
- (33) Ryu, N.; Okazaki, Y.; Pouget, E.; Takafuji, M.; Nagaoka, S.; Ihara, H.; Oda, R. Fluorescence Emission Originated from the H-aggregated Cyanine Dye with Chiral Gemini Surfactant Assemblies Having a Narrow Absorption Band and a Remarkably Large Stokes Shift. Chem. Commun. 2017, 53, 8870-8873.
- (34) Crawford, A. G.; Dwyer, A. D.; Liu, Z.; Steffen, A.; Beeby, A.; Palsson, L. O.; Tozer, D. J.; Marder, T. B. Experimental and Theoretical Studies of the Photophysical Properties of 2- and 2,7-Functionalized Pyrene Derivatives. J. Am. Chem. Soc. 2011, 133, 13349-13362.
- (35) Lee, Y. O.; Pradhan, T.; Choi, K.; Choi, D. H.; Lee, J. H.; Kim, J. S. Electrogenated chemiluminescence of N,N-dimethylamino functionalized tetrakis(phenylethynyl)pyrenes. Tetrahedron 2013, 69, 5908-5912.
- (36) Chi, W.; Yin, W.; Qi, Q.; Qiao, Q.; Lin, Y.; Zhu, Z.; Vijayan, S.; Hashimoto, M.; Udayakumar, G.; Xu, Z.; Liu, X. Ground-State Conformers Enable Bright Single-Fluorophore Ratiometric Thermometers with Positive Temperature Coefficients. Mater. Chem. Front. 2017, 1, 2383-2390.
- (37) Wu, C.; Shi, C.; Zheng, Y.; Zhang, J.; Wang, Y.; Sun, N.; Wang, Q.; Lu, Z.-H. Multifunctional Luminophores with Dual Emitting Cores: TADF Emitters with AIE Properties for Efficient Solution- and Evaporation-Processed Doped and Non-doped OLEDs. Chem. Eng. J. 2022, 431, 133249.
- (38) Zeng, J.; Qiu, N.; Zhang, J.; Wang, X.; Redshaw, C.; Feng, X.; Lam, J. W. Y.; Zhao, Z.; Tang, B. Z. Y - Shaped Pyrene - Based Aggregation - Induced Emission Blue Emitters for High - Performance OLED Devices. *Adv. Opt. Mater.* **2022**, 2200917.
- (38) SAINT and APEX 2. Software for CCD diffractometers 2015.
- (39) Sheldrick, G. M. A short history of SHELX Acta Crystallogr. A 2008, 64, 112.
- (40) Crawford, A. G.; Liu, Z.; Mkhaliid, I. A.; Thibault, M. H.; Schwarz, N.; Alcaraz, G.; Steffen, A.; Collings, J. C.; Batsanov, A. S.; Howard, J. A.; Marder, T. B. Synthesis of 2- and 2,7-

Functionalized Pyrene Derivatives: an Application of Selective C-H Borylation. *Chem. Eur. J.* 2012, 18, 5022-5035.

- (41) Coventry, D. N.; Batsanov, A. S.; Goeta, A. E.; Howard, J. A.; Marder, T. B.; Perutz, R. N. Selective Ir-catalysed Borylation of Polycyclic Aromatic Hydrocarbons: Structures of Naphthalene-2,6-bis(boronate), Pyrene-2,7-bis(boronate) and Perylene-2,5,8,11-tetra(boronate) Esters. *Chem. Commun.* 2005, 2172-2174.
- (42) Zeng, J.; Wang, X.; Song, X.; Liu, Y.; Liao, B.; Bai, J.; Redshaw, C.; Chen, Q.; Feng, X. Steric Influences on the Photophysical Properties of Pyrene-Based Derivatives; Mechanochromism and their pH-responsive Ability. *Dyes Pigm.* 2022, 200, 110123.
- (43) Xia, Z.; Khaled, O.; Mouries-Mansuy, V.; Ollivier, C.; Fensterbank, L. Dual Photoredox/Gold Catalysis Arylative Cyclization of o-Alkynylphenols with Aryldiazonium Salts: A Flexible Synthesis of Benzofurans. *J. Org. Chem.* 2016, 81, 7182-7190.

## Table of Content



- ✓ **One-pot synthesis**
- ✓ **red-emission in solid state**
- ✓ **Two-Photon Absorption**
- ✓ **Tunable TPA cross section value**
- ✓ **Structure-Property Relationship**